Assessing the population genetic structure and demographic history of *Anopheles gambiae* and *An. arabiensis* at island and mainland sites in Uganda: Implications for testing novel malaria vector control approaches.

Rita Mwima [1,2], Tin-Yu J. Hui [3], Edward Lukyamuzi [1], Marilou Bodde [4], Alex Makunin [4], Krystal Birungi[1], Martin Lukindu[1], Ann Nanteza[2], Dennis Muhanguzi[2], Mara Lawniczak [4], Austin Burt [3], Jonathan K. Kayondo [1]

1 Department of Entomology, Uganda Virus Research Institute (UVRI), Entebbe, Uganda.

2 Department of Biotechnical and Diagnostic Sciences, College of Veterinary Medicine, Animal Resources and Biosecurity (COVAB), Makerere University, Uganda.

3 Silwood Park Campus, Department of Life Sciences, Imperial College London, Ascot, UK.

4 Tree of Life, Wellcome Sanger Institute, Wellcome Genome Campus, Hinxton, Cambridgeshire, UK.

*Corresponding author

Email: jkayondo@gmail.com

Abstract

Despite substantial investments in malaria control, the disease remains a major burden in sub-Saharan Africa, particularly Uganda. Novel tools such as gene drive systems are being developed to suppress malaria vector populations, but their deployment requires detailed knowledge of mosquito population genetics.

We assessed the genetic structure, diversity, and demographic history of *Anopheles gambiae* and *Anopheles arabiensis* from six sites in Uganda: three islands in Lake Victoria and three mainland sites. A total of 2918 *Anopheles gambiae* and 173 *Anopheles arabiensis* were genotyped using targeted amplicon sequencing of 62 loci across coding and non-coding regions of the genome.

Population structure analyses revealed clear separation between the two species but little differentiation within each species across sites. Pairwise *F*ST values among *An. gambiae* populations were low (0.00054–0.028) but often significant, with mainland populations showing higher connectivity and island populations exhibiting greater isolation. *Anopheles arabiensis* mainland populations showed no statistically significant differentiation, suggesting panmixia. Principal Component Analysis and Bayesian clustering similarly distinguished species-level structure but no obvious substructure within sites.

Mainland *An. gambiae* populations displayed higher nucleotide diversity than island populations, while *An. arabiensis* showed the lowest diversity overall. Tajima's D values were negative across sites, consistent with recent population expansions. Effective population size estimates indicated small populations at the islands (146 to 249) compared to large mainland populations (4,054 to 8,190).

These findings demonstrate strong genetic differentiation between *Anopheles gambiae* and *Anopheles arabiensis*, and subtle but meaningful structure between island and mainland *Anopheles gambiae* populations. The reduced diversity and small effective population sizes at island sites suggest stronger genetic drift and limited gene flow, in contrast to the highly connected mainland populations.

For malaria control, this contrast has direct implications. High connectivity among mainland populations may facilitate the spread of insecticide resistance alleles, while island populations, with their relative isolation and smaller sizes, may serve as suitable sites for contained field trials of gene drive strategies. This study highlights how geographic and ecological factors shape mosquito population structure and provides critical evidence for the design and monitoring of genetic-based vector control interventions.

Keywords: Gene drive systems, insecticide resistance, field trial sites, gene flow.

Background

Despite enormous efforts in malaria control, the disease remains a global burden, especially in the Sub-Saharan Africa. This is because of the exceptionally adaptive dynamics of *Anopheles* mosquitoes together with other factors that include insecticide resistance, drug resistance, limited access to healthcare, and environmental and socio-economic challenges [1,2].

In 2024, the World Health Organisation (WHO) reported about 200 million cases and 600,000 deaths [3]. Recent years have shown a persistently high malaria burden with case and mortality numbers remaining largely stable from 2021 to 2023, underscoring the health challenge the disease poses, despite the control efforts in place [4,5]. Sub-Saharan Africa carries the greatest burden globally, accounts for 94% of all malaria cases and 96% of all deaths [3]. Uganda, in particular, experiences a heavy burden due to malaria, ranking third in the number of malaria cases worldwide in 2023 and contributing 5% of the global burden [3].

The fight against malaria is increasingly challenged by the evolving resistance of parasites to antimalarial drugs and of mosquitoes to various insecticides, coupled with the partial efficacy of current control methods [3,6–9]. To achieve malaria elimination and eradication will thus require new products and interventions to be used in tandem with the already existing tools [10]. One promising strategy is the mosquito gene drive technology, a genetic engineering approach that biases the inheritance of a specific gene or trait, causing it to spread rapidly through a population over generations, capable of spreading into an entire population from low initial frequencies [11,12] to either suppressing mosquito populations by reducing their fertility or modifying them so they are unable to transmit the malaria parasite [13].

Significant advancements have been made so far in target gene identification, gene construct development, and genome sequencing of the major malaria mosquito populations [14–16].

Despite the proof-of-concept mosquito transformation studies done in laboratories and the idententification of candidate gene drive systems [17–19], there is need to advance for further field trials such that product feasibility and efficacy can be evaluated. Furthermore, detailed population genetic assessments must be done systematically before deploying any proposed trial or intervention [20]. Information on population genetic structure and gene flow within a vector species provides a basis for modeling the impact of trial intervention and in trial design and helps select suitable locations for field trials, given that, Ideally, these locations should have limited gene flow with surrounding populations [21,22].

In Uganda, the geographic and genetic isolation of lacustrine *An. gambiae* island populations from mainland renders them suitable candidate sites for initial testing of mosquito gene drive systems [15]. Conversely, regions with high gene flow are significant for gene drive strategies because they provide high connectivity among populations and enhance the potential for rapid and extensive spread of gene drive elements, which is essential for effective malaria vector control on a broader scale [23–25].

Knowledge of A*n. gambiae* and *An. arabiensis* genetic diversity, structure, and population sizes at island and mainland sites will provide critical insights into the genetic differences and dynamics at the target field sites, thereby aiding in the design of interventions and monitoring their efficacy [21,26,27]. Several studies have examined the structure of *An. gambiae* at the island and mainland sites in Uganda [28–30], but there are no studies that compare the population structure of both *An. gambiae* and *An. arabiensis*, despite their known sympatric occurrence in many regions [31,32]. These two species are closely related members of the *Anopheles gambiae* complex, sharing overlapping habitats and breeding sites, which creates opportunities for gene flow and introgression that could impact important traits such as

insecticide resistance and vector competence [21,33]. Therefore, assessing their population structure and potential gene flow jointly, is critical to understanding their ecological interactions and for optimizing vector control strategies. *Anopheles arabiensis* from the lacustrine islands is often excluded from further analysis due to their limited numbers in the mosquito collections done to date [26,27,34], and yet anecdotal observations suggest that the islands on Lake Victoria may have an increasing presence of *An. arabiensis* alongside *An. gambiae*, suggesting a shift in species composition and complexity of malaria vector species in these areas (personal communication). The explanation for this could be This could be, microclimatic conditions that result in increased density of a given species in areas where their numbers were previously very low [35–37].

This study employed population genetics approaches like meansures of genetic diversity, differentiation and gene flow estimates to characterize the population structure of *An. gambiae* and *An. arabiensis* across selected island and mainland sites in Uganda. This analysis utilised amplicon data generated from an amplicon panel specifically designed for species identity.

Methods

Mosquito sampling

Mosquito collections were conducted from six sites including three mainland sites (Kayonjo, Katuuso, Kibbuye) and three island (Bugiri, Kiimi, Kansambwe) sites (Figure 1). These sites were chosen based on several criteria: (1) high malaria endemicity, (2) a high density of the target mosquito species (*An. gambiae* complex), (3) a distance from urban areas with a mix of permanent and temporary housing, (4) a moderate population size (between 500-1000 residents), (5) minimal ongoing malaria vector control activities, and (6) a cooperative and welcoming local community. Kibbuye and Katuuso villages are situated in Mukono district and Kayonjo village in Kayunga district (Figure 1), which are each approximately 50km North West of the capital city, Kampala. The lacustrine island sites are situated within Lake Victoria in Uganda and are connected by ship and ferry service to the Ugandan mainland. Figure 1B shows how far each site is from another.

A

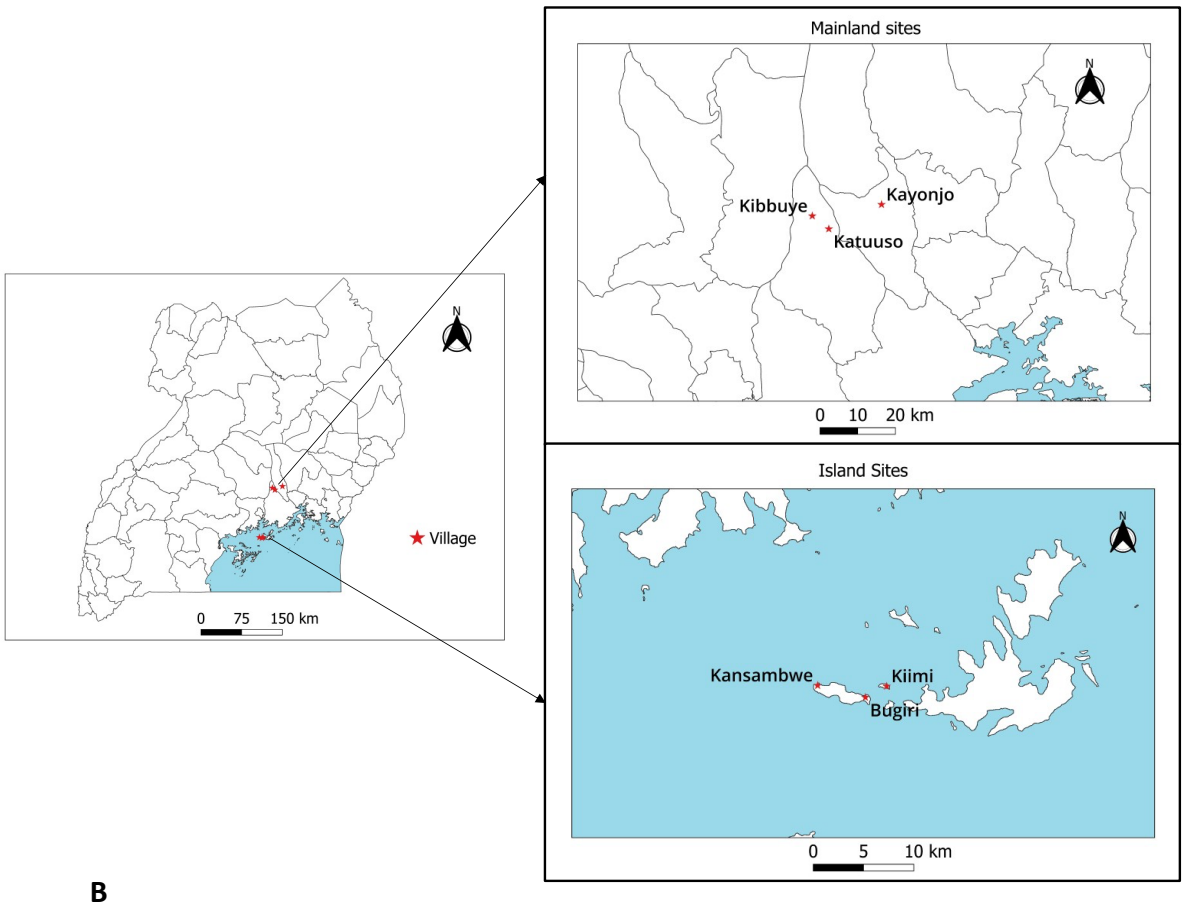
Mainland sites
Kibbuye
Kayonjo
Katuuso
0 10 20 km
Village
0 75 150 km
Island Sites
Kansambwe
Kiimi
Bugiri
0 5 10 km

B

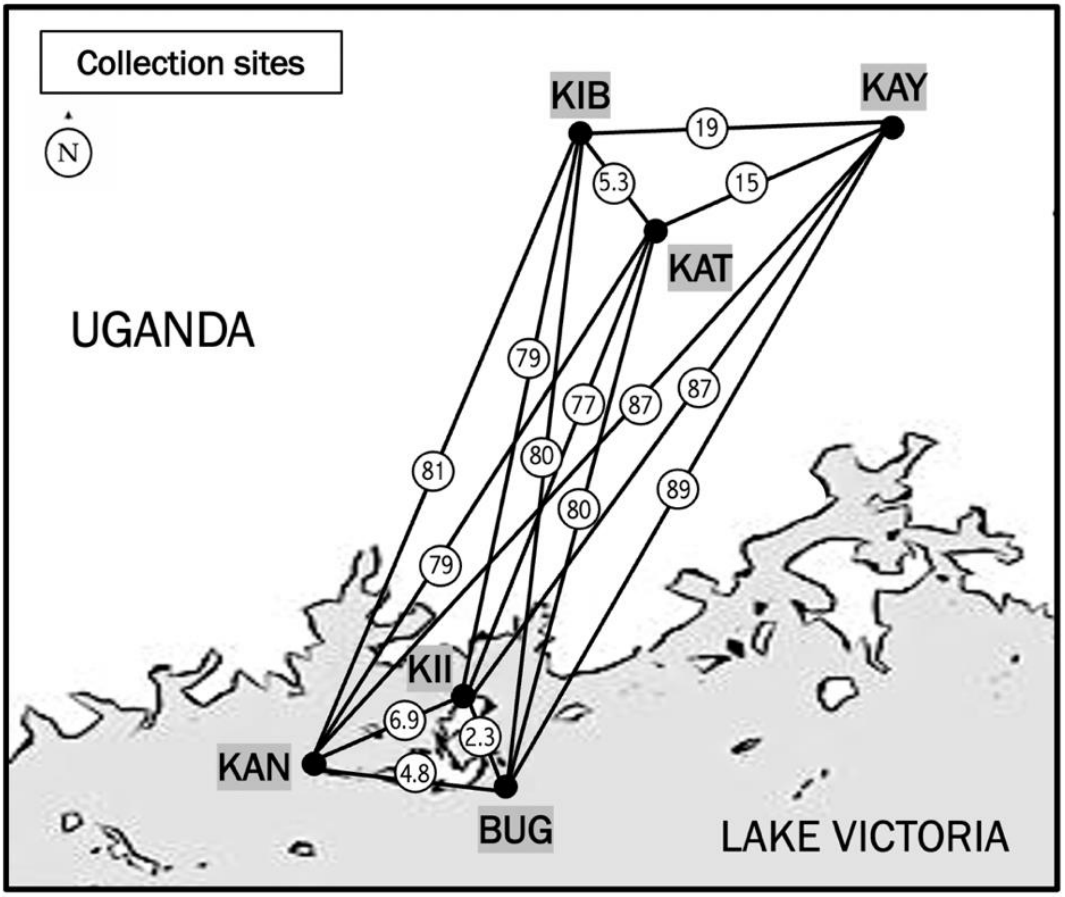
Collection sites
N
KIB
KAY
KAT
KII
KAN
BUG
UGANDA
LAKE VICTORIA
19
5.3
15
79
77
87
87
81
80
89
80
79
6.9
2.3
4.8

144 **Figure 1A**: Map showing the location of the 3 mainland and 3 island study sites in Uganda, **B:**
145 Distances (in kilometers and circled) between sites. KAY= Kayonjo, KIB = Kibbuye, KAT =
146 Katuuso, KII = Kiimi, KAN = Kansambwe, BUG = Bugiri.

147 Collections done on the islands and mainlands were part of routine mosquito collections done
148 by the Department of Entomology at the Uganda Virus Research Institute. On the islands,
149 collections were done from April 2013 to April 2016, and on the mainland from January 2016
150 to December 2018. Adult mosquitoes were sampled indoors and outdoors using human
151 landing catches (HLC), pyrethroid spray catches (PSC), indoor and outdoor aspirators, and
152 catch basin traps (CBT). All mosquitoes were morphologically identified using the *Anopheles*
153 morphological identification keys [38] and then stored in 80% ethanol for subsequent
154 molecular analysis. For this study we kept only *An. gambiae* and *An. arabiensis* mosquitoes,
155 although some *An. funestus*, *An. maculipalpis*, and *An. coustani* were also collected (but
156 excluded from this analysis).

157 **Genomic DNA extraction**

158 A total of 3515 whole mosquito samples, each stored in a 96-well plate of 80% ethanol, were
159 shipped to the Wellcome Sanger Institute, United Kingdom, for DNA extraction and amplicon
160 sequencing [16,39]. In brief, DNA extraction was completed by removing the ethanol from
161 each specimen, adding 100 ul of lysis buffer C to each, and incubating plates at 56 ^{0}C for
162 overnight, allowing preservation of specimens for further examination [16]. DNA from each
163 mosquito was then subjected to a single Polymerase Chain Reaction (PCR) reaction containing
164 a 64 primer pair plex [16]. Each reaction then went into a second PCR to add indexing primers.
165 Eight plates of mosquitoes were pooled for a single MiSeq library [16].

166 Using the ANOpheles SPecies and Plasmodium (ANOSPP) panel of 64 phylogenetically
167 informative and highly variable "amplicon loci" of which 62 target the Anopheles nuclear
168 genome and the other 2 targeting the Plasmodium mitochondria (note: these amplicon loci
169 are of ~160 base pairs or "sites" long in downstream analyses), the generated sequence data
170 enabled species identification, detection of Plasmodium, hybrid or contaminated samples,
171 and identification of cryptic species [16]. This panel consists of 62 nuclear loci distributed
172 across the *Anopheles* genome, comprising 17 coding (exonic), 22 intronic, and 23 intergenic
173 (non-coding) regions [16]. (For all other details regarding the sequencing techniques, and the
174 functions of the 62 amplicon loci, please refer to the original publication [16,39]).

175 A Variational Autoencoder (VAE), which is a machine learning approach that identifies
176 patterns in high-dimensional data by compressing it into a lower-dimensional representation
177 [40] was used to distinguish between closely related species [39].

178 **Bioinformatics processing**

179 The raw reads from the generated sequence data for the confirmed *An. gambiae* and *An*.
180 *arabiensis* were processed using AmpSeeker, an open-source computational pipeline which
181 includes quality filtering, primer trimming, alignment to the reference genome file
182 (VectorBase-59_AgambiaePEST_Genome.fasta), and variant calling (e.g with BWA, bcftools).
183 [40]. AmpSeeker is a Snakemake-based workflow designed for Illumina amplicon sequencing
184 data [41]. Using this pipeline, samples were filtered based on sequencing depth,
185 heterozygosity and principal component outlier analysis to remove low-quality or anomalous
186 samples, before downstream analyses like population structure and gene flow were
187 performed [41].

The resulting raw variant call format (VCF) file contains variant calls across all samples and comprises a total of 12,412 sites (inclusive of insertions and deletions (indels), primer regions, fixed and polymorphic sites). Subsequent subsetting was performed on the VCF file based on the metadata information, which provided details about the mosquito samples, including individual sample IDs, species, collection location, collection period, and season among others. In the filtering process, indels were removed, resulting in 9,890 remaining sites. These sites were distributed across the genome as follows: X (n = 952), 2L (n = 1881), 2R (n = 2815), 3L (n = 1615), 3R (n = 2627). The minor allele frequency (maf) spectrum between 0 and 2% is shown in Figure 2, and the number of alleles per locus (from fixed to quadriallelic) is in Figure 3. Our downstream analyses were based on these 9,890 sites with potential further filtering, such as according to maf and missing values (Using only biallelic SNPs).

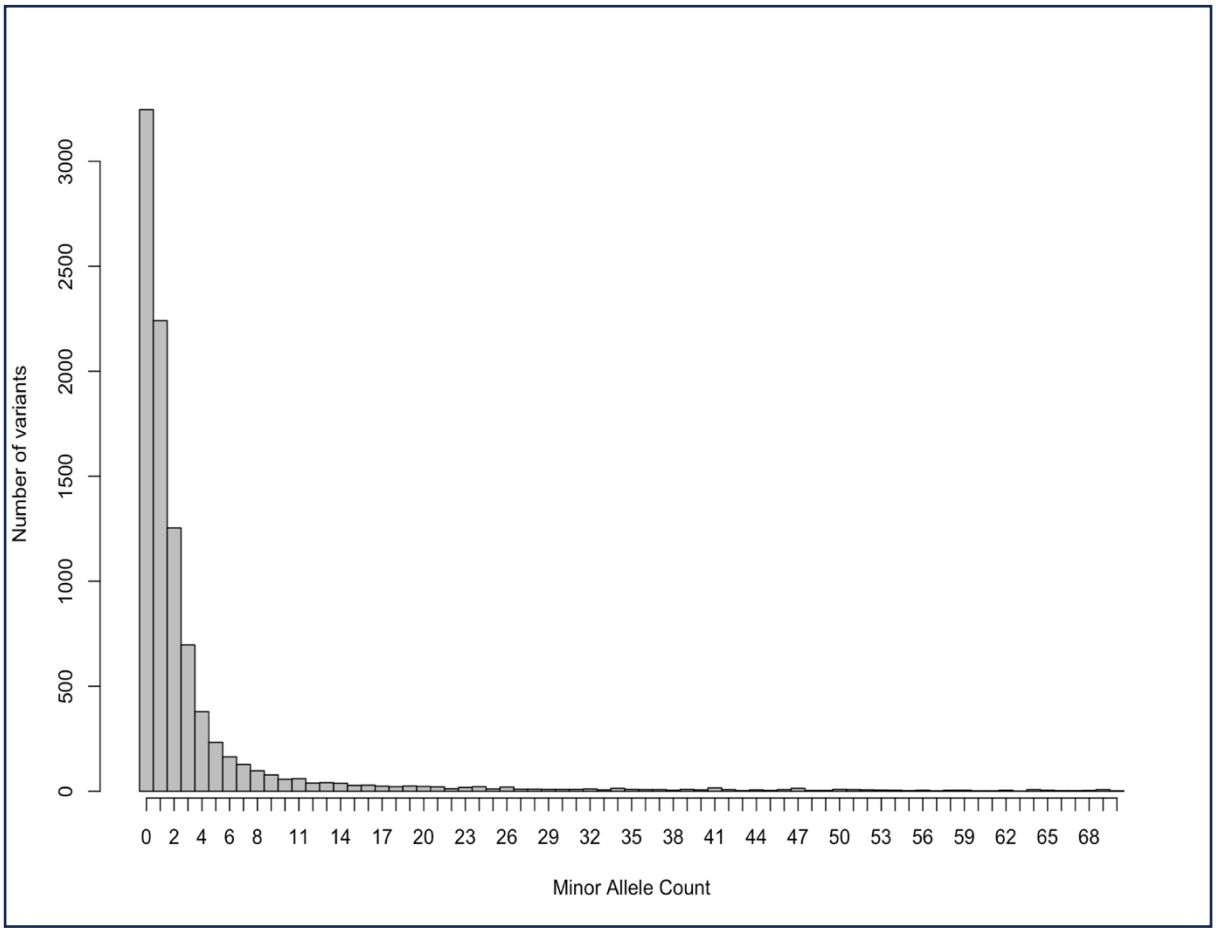

208 **Figure 2:** Minor allele frequency (MAF) spectrum between 0 and 2% (for the whole dataset).

209

210
211
212
213
214
215
216
217
218
219
220
221
222

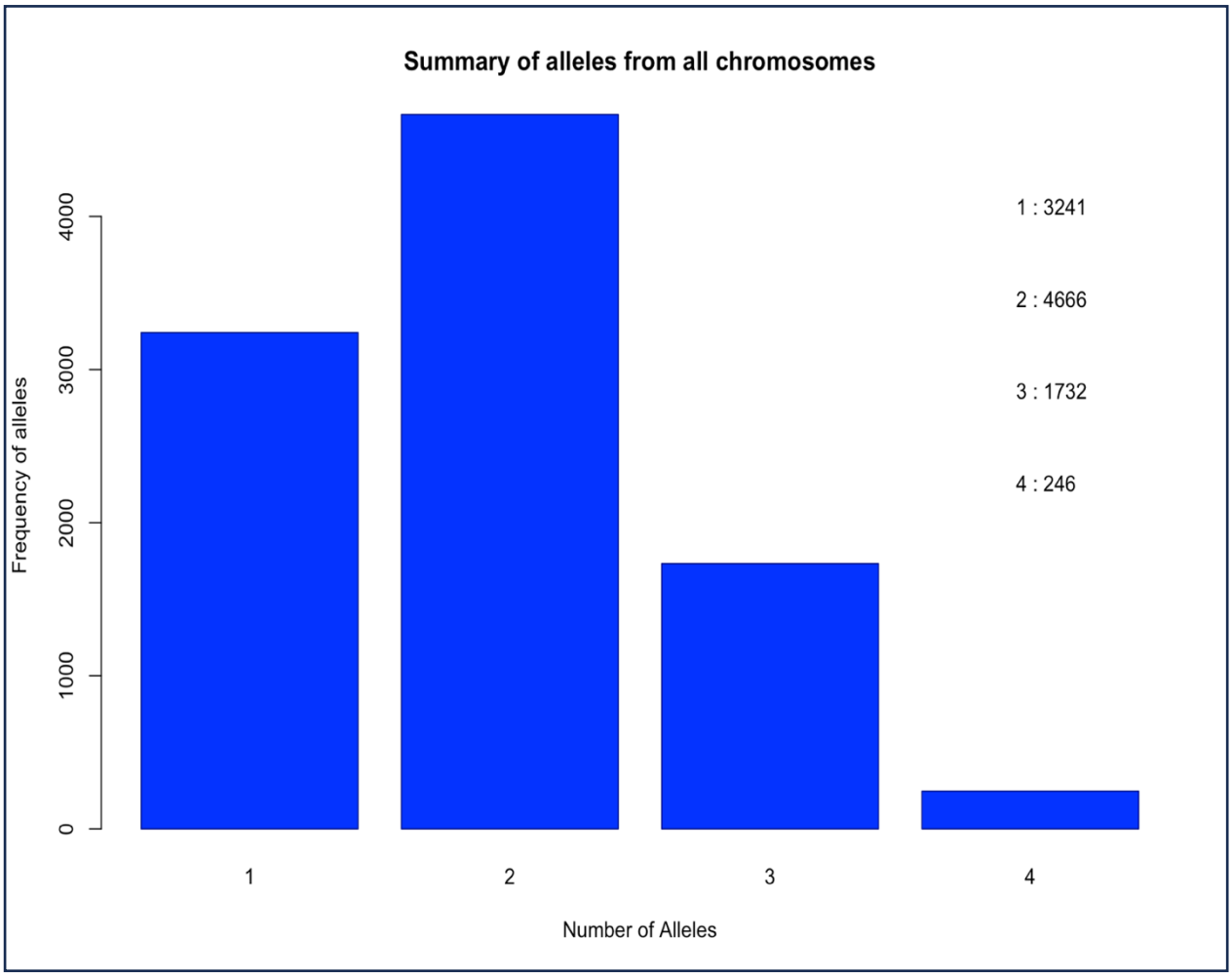

223 **Figure 3**: Summary of the number of alleles per site from all chromosomes. 9890 sites are
224 included. The 5 sites with 0 alleles are missing values in all our *An. gambiae* and *An. arabiensis*
225 samples and were excluded from the graph.

226 **Population genomic analysis**

227 ***Population structure***

228 The following methods were used to describe population structure: (1) F_{ST} between and within
229 pairs of populations using version 1.3.23 of the Popkin package in R [42,43], (2) Principal

230 Components Analysis (PCA) using version 3.6.2 of the prcomp package in R [42,43], and (3)
231 Bayesian clustering analysis with STRUCTURE v2.3.4 [44]. Average pairwise Hudson's F_{ST} was
232 calculated using the fst_hudson_pairwise function of the Popkinsuppl package [45], after
233 which standard errors were computed using the leave-one-out approach that is a specific form
234 of the jackknife resampling method [46–48]. Z-scores were then computed by dividing the
235 estimated FST by its standard error. These Z-scores were used to assess the significance (P-
236 values) of the F_{ST} values. The P-values are derived from the Z_scores by comparing them
237 against the standard normal distribution, which allows for determining the probability of
238 observing such F_{ST} values under the null hypothesis of no differentiation between populations
239 [48]. All the *An. gambiae* collected from the same location were considered as a population,
240 while all 173 *An. arabiensis* were grouped as the seventh population. The *An. arabiensis*
241 samples were grouped as a single population in the analysis because their sizes per site were
242 too small to conduct statistically robust population-level analyses individually. Grouping all *An.*
243 *arabiensis* samples increased the analytical power to detect genetic patterns and structure
244 across the mainland populations, providing a more reliable overview of their genetic
245 differentiation.

246 For pairwise F_{ST}, we used biallelic sites with 10% missing data from within the 3L chromosome
247 with maf >=1%, while for PCA, we first considered all chromosomes and thereafter only the
248 3L arm, because, unlike other autosomes, it does not carry chromosomal inversions that
249 suppress recombination and could confound analyses of population structure. To investigate
250 the role of geographic distance in shaping genetic differentiation, we ran a Mantel test to test
251 for isolation by distance (IBD) between populations by combining Euclidean geographic
252 distances (calculated from geographic coordinates) and genetic distances based on 9999

253 permutations using GenAlEx 6.51b2 [49,50]. For *An. arabiensis* populations, the same F_{ST} and
254 Mantel tests were also conducted using the 3L chromosome arm biallelic SNPs but only for
255 the three mainland sites. The islands were left out because of their small sample sizes (Table
256 1). PCA was performed in R v4.3.1 with the prcomp() function [51,52], first for biallelic SNPs
257 from all chromosomes and then for the 3L chromosome arm.

258 **Table 1.** The number of confirmed *An. gambiae* and *An. arabiensis* samples across six
259 collection sites

	Bugiri †	Kiimi †	Kansambwe †	Kayonjo	Katuuso	Kibbuye	Total
An. gambiae	28	258	294	1178	450	710	2918
An. arabiensis	2	0	3	51	39	78	173
Total	30	258	297	1229	489	788	3091

260 † Denotes island sites.

261 We looked at doubletons, defined as loci with exactly two copies of the minor allele in a
262 biallelic site. A contingency table of observed counts of heterozygous doubleton pairs across
263 populations was constructed, and the expected counts were calculated based on sample size
264 proportions to assess population structure. Populations were grouped into three categories,
265 *arabiensis* (*An. arabiensis*), *mainland_gam* (mainland *An. gambiae*), and *Island_gam* (island
266 *An. gambiae*), and a chi-square test was conducted to compare observed and expected counts
267 to detect significant population structure.

268 To find the optimal number of clusters (K) in STRUCTURE (using model with no admixture), we
269 conducted 20 independent runs for each K (from 2-8), using a burn-in value of 100,000
270 iterations followed by 100,000 repetitions [44]. Then K was determined using the Delta K
271 method of Evanno et al. [53], following which CLUMPAK was used to construct a graphical

272 representation of the genetic structure of the 3091 (both *An. gambiae* and *An. arabiensis*)
273 mosquito samples [54]. In this analysis, we randomly chose one variable site per amplicon
274 locus from the 2R, 3R, and 3L chromosome arms to minimise genetic linkage, with the
275 constraint that maf≥1%.

276 ***Genetic diversity and Ne***

277 To assess the genetic diversity per population, we calculated the overall nucleotide diversity
278 (p) as well as individually for the 6 *An. gambiae* and 3 mainland *An. arabiensis* populations for
279 each chromosome arm [55] using VCF files without missing data. Deviation from the standard
280 neutral model was tested using Tajima's D, which was performed for each site and
281 chromosome to examine population expansion [56]. Tajima's D and nucleotide diversity were
282 computed using the Pegas package in R [57]. Estimates of contemporary Ne were attained
283 using the linkage disequilibrium (LD) based method LDNe [58] of NeEstimator v.2.01 [59]. We
284 randomly chose one site per amplicon locus from chromosomes 3R and 3L with maf≥1% to
285 avoid tight linkage. We similarly individually computed nucleotide diversity, Tajima's D and
286 contemporary Ne for individual mainland *An. arabiensis* populations.

287

288

289

290

291

292

293

294

295 **Results**

296 **Genetic differentiation (F_{ST})**

297 2918 samples were confirmed as *An. gambiae* and 173 as *An. arabiensis*. These individuals
298 and their resulting amplicon data were our subjects for downstream population genetic
299 analyses, and Table 1 summarises their distribution across the six collection sites. The average
300 pairwise Hudson's F_{ST} is found in Table 2A. All pairwise comparisons produced low F_{ST} values
301 (0.00054-0.028), except between the "outgroup" *An. arabiensis* and any *An. gambiae*
302 populations. Among *An. gambiae* mainland populations, pairwise F_{ST} values were very low
303 (0.00054-0.0016, indicating minimal genetic differentiation, and similarly, low F_{ST} values were
304 observed between Bugiri (island) and the other two islands (Kiimi and Kansambwe),
305 suggesting significant gene flow. The highest F_{ST} values occurred between Kansambwe (island)
306 and all the mainland sites (Kayonjo, Katuuso and Kibbuye) (island vs mainland), and between
307 Kiimi and Kansambwe (island vs island), implying restricted gene flow in these comparisons
308 (Table 2A). The pairwise F_{ST} values between Bugiri (island) and all the other sites, Kayonjo
309 (mainland) and Katuuso (mainland), Kiimi (island) and Katuuso(mainland) and Kiimi (island)
310 and Kibbuye (mainland) were low and non-significant ($z < 1.96$, $P > 0.05$). We then calculated
311 pairwise F_{ST} values among the mainland *An. arabiensis* populations (Table 2B), and low and
312 statistically nonsignificant pairwise F_{ST} values (-0.0014994 - 0.00785541) were mostly
313 recorded. The F_{ST} value between Katuuso (mainland) and Kibbuye (mainland) was negative,
314 which is interpreted as no differentiation.

315

316

317

318

	BUGIRI †	KIIMI †	KANSAMBWE †	KAYONJO	KATUUSO	KIBBUYE	*An. arabiensis*
BUGIRI †	0	0.6796089	0.5914296	1.762527	1.628254	1.47858	4.361302*
KIIMI †	0.00287	0	4.631849*	1.977574*	1.943631	1.78073	4.360677*
KANSAMBWE †	0.00272	0.02123	0	3.189523*	3.041091*	3.916723*	4.041615*
KAYONJO	0.00995	0.01199	0.02715	0	1.204753	1.991724*	3.779667*
KATUUSO	0.01201	0.01483	0.02841	0.00054	0	2.439927*	3.826917*
KIBBUYE	0.01033	0.01740	0.02433	0.00109	0.00163	0	3.737203*
An. arabiensis	0.21710	0.20209	0.26279	0.22654	0.23330	0.20902	0

Table 2: Pairwise F_{ST} statistics

A. *An. gambiae* & *An. arabiensis*

B. *An. arabiensis*

	KAYONJO	KATUUSO	KIBBUYE
KAYONJO	0	1.817574	0.09362245
KATUUSO	0.00785541	0	-1.070926
KIBBUYE	0.00018109	-0.0014994	0

(A) Pairwise FST from the 3L chromosome arm for the six *An. gambiae* populations, with the 173 *An. arabiensis* grouped as the seventh population. (B) Pairwise FST among the three *An. arabiensis* populations. For both tables, the lower left triangle in each table shows average Hudson's F_{ST} values between each population pair, while the upper right triangle shows the z-

328 scores for each F_{ST} value calculated via a block-jackknife method. The values with * indicate

329 significant F_{ST} values ($z > 1.96$, $p < 0.05$). † Denotes island sites.

330 The pairwise F_{ST} values for *An. gambiae* were plotted against geographic distances to

331 investigate the strength of isolation by distance [50,60], and the correlation was not

332 statistically significant (Figure 4, P = 0.052).

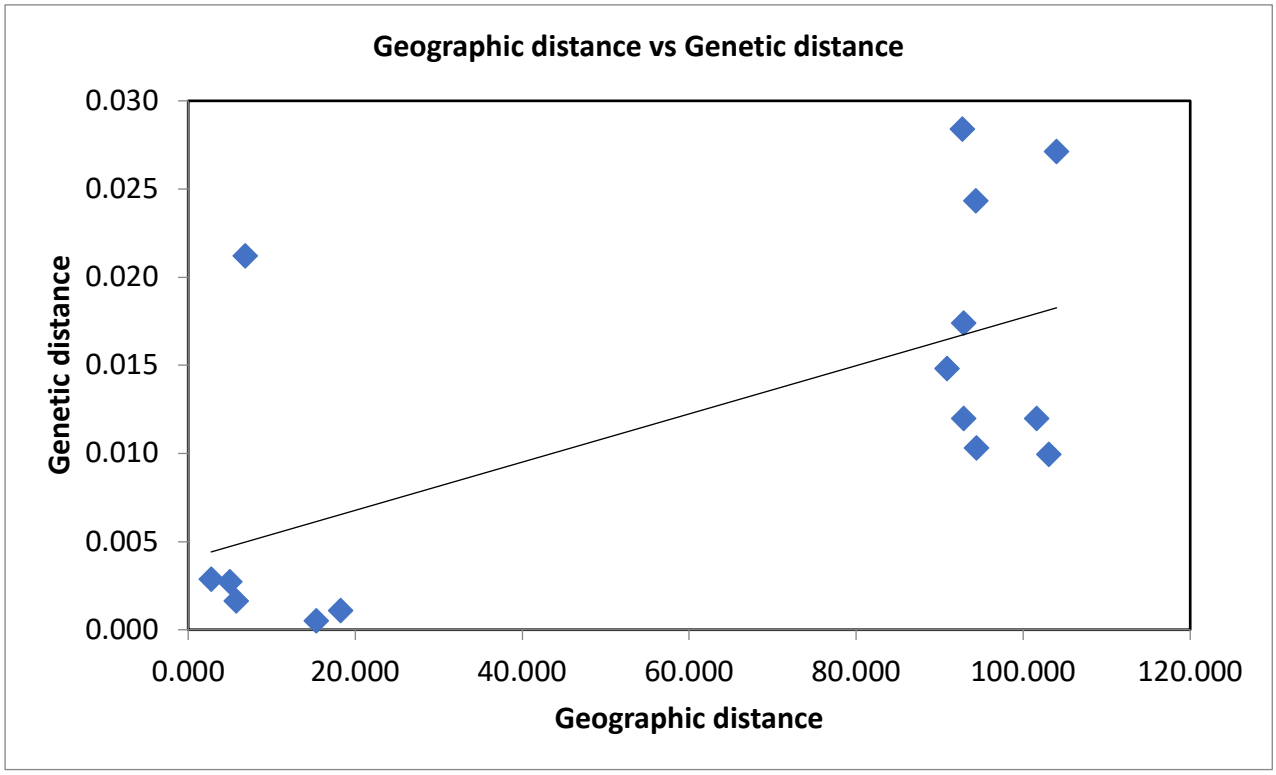

333

334 **Figure 4:** F_{ST} versus geographical distance (km) for *An. gambiae*. FST values were extracted

335 from Table 2. The figure shows a positive slope with no significant correlation between the

336 genetic and geographic distances, P = 0.052

337 **PCA**

338 PCA visualises how the individuals were genetically clustered within and between collection

339 sites. Analysis using all biallelic sites of all chromosome arms of all *An. gambiae* and *An.*

340 *arabiensis* samples showed clustering into two distinct groups in accordance with each
341 species' genetic difference (Figure 5A). The 3L chromosome arm from both *An. gambiae* and
342 *An. arabiensis* also showed species-specific clustering (Figure 5B) and using chromosome 3L
343 sites of only *An. gambiae*, no geographical clustering of individuals was observed (Figure 5C).

344 **A**

345 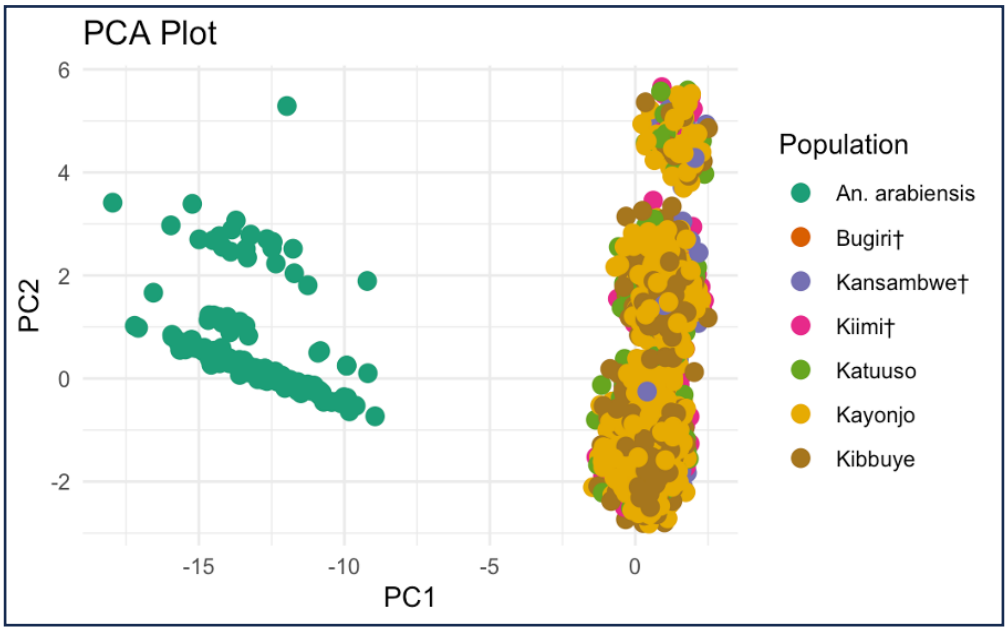

353

354 **B**

355 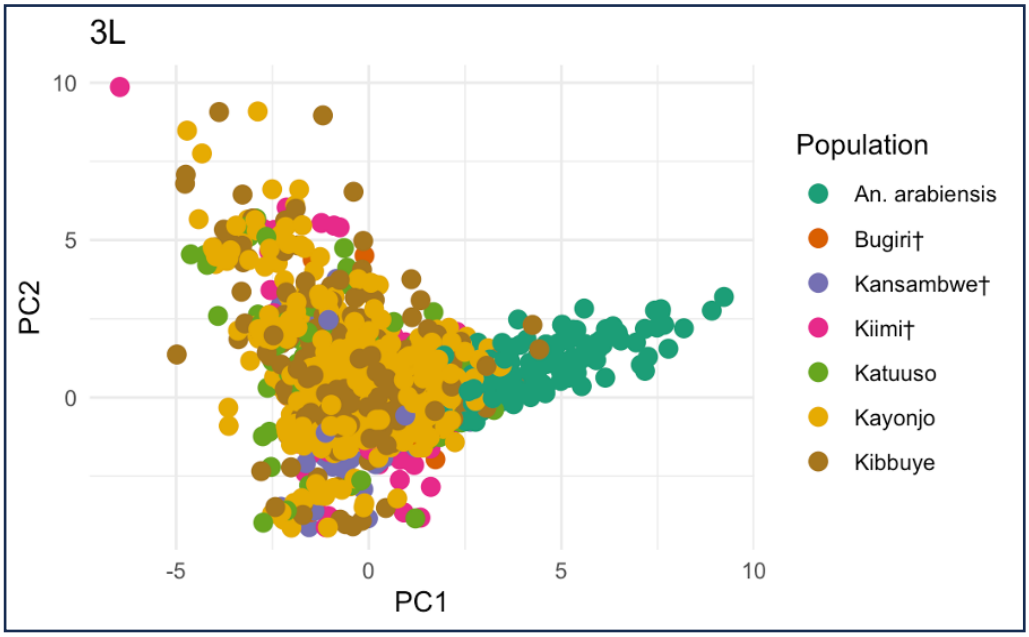

363

364

365 **C**

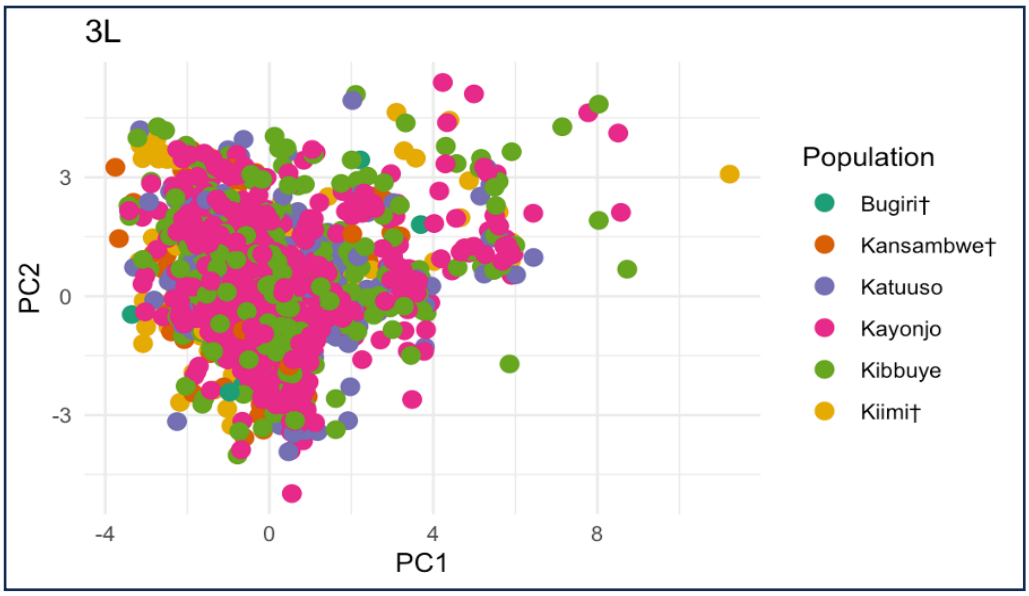

366 367 368 369 370 371 372 373

374 **Figure 5 A:** Principal component analysis of all chromosome arms of *An. gambiae* (island and
375 mainland sites) and *An. arabiensis*, **B:** The PCA was calculated from the 3L chromosome arm
376 of *An. gambiae* and *An. arabiensis* individuals, and **C**: The PCA was calculated from the 3L
377 chromosome arm of only *An. gambiae* individuals. † Denotes island sites.

378 **Allele sharing in doubleton variants**

379 839 pairs of doubletons were discovered. We calculated the expected counts based on sample
380 size proportions to account for the distribution of the observed heterozygote doubleton pairs
381 under a null hypothesis assuming no population structure. Because of the limited resolution
382 available to distinguish between individual populations in our dataset, we reduced the original
383 6+1 (Bugiri, Kiimi, Kansambwe, Kayonjo, Katuuso, Kibbuye, and *An. arabiensis*) population
384 groups into three broader categories: *arabiensis*, *island_gam*, and *mainland_gam*. In this way,
385 more robust statistical comparisons and interpretations of allele sharing across major
386 population segments could be made. The reduction from 6+1 populations to three groups

387 improved statistical power and provided insights into gene flow dynamics across the major
388 geographic and species categories of interest.

389 There were significant deviations between observed and expected pairwise counts of
390 doubleton pairs in the three groups: *arabiensis*, *island_gam*, and *mainland_gam*. The
391 observed pairwise counts of heterozygotes within and between population groups highlight
392 actual genetic similarities, while the expected pairwise counts reflect the hypothetical
393 distribution of pairings in the absence of genetic structuring.

394 When we considered within-group genetic structuring (Table 3), the *mainland_gam* group
395 showed a significantly higher within-group count of heterozygous pairs than expected (682
396 observed vs. 480 expected), which suggests a higher-than-anticipated allele sharing or pairing
397 frequency within this group. The *island_gam* group showed a lower-than-expected level of
398 allele sharing (2 observed vs. 29.54 expected), suggesting limited gene flow with other
399 populations, while, the *arabiensis* group showed moderated within-group genetic isolation
400 (15 observed versus 2.63 expected counts), suggesting that it is a relatively closed genetic pool
401 with reduced gene flow to other populations.

402 **Table 3:** Allele sharing in doubleton variants

403 A. Observed counts

	arabiensis	*island_gam*	*mainland_gam*
arabiensis	15	4	102
island_gam	NA	2	34
mainland_gam	NA	NA	682

404

B. Expected counts

	arabiensis	*island_gam*	*mainland_gam*
arabiensis	2.628186	17.62252	71.03699
island_gam	NA	29.54064	238.1587
mainland_gam	NA	NA	480.01296

Within and between group counts

When we considered between-group genetic structuring, the observed gene flow between *arabiensis* and *mainland_gam* groups (102 observed versus 71.04 expected counts) indicates occasional genetic exchange, which could be as a result of ancestral similarities. *island_gam* versus *mainland_gam* have significantly fewer pairs than expected (34 pairs versus an expectation of 238.16 pairs), suggesting restricted gene flow between the two geographic sites. The *arabiensis* versus *island_gam* groups had significantly fewer pairs than expected (4 pairs versus an expectation of 17.62252 pairs), suggesting restricted gene flow between the two groups.

Bayesian clustering analysis

Based on the log-likelihood values and the DeltaK plot, K=3 was the optimal number of evolutionary clusters (Figure 6A). Therefore, the six *An. gambiae* populations and pooled *An. arabiensis* were substantially admixed at K = 3 (K = 3 best explains the genetic variance present between all the sites). Upon close inspection of the results from the Bayesian cluster analysis(Figure 6B), three significant genetic clusters were identified: (1) pooled *An. arabiensis* individuals, (2) island *An. gambiae* individuals, (3) mainland *An. gambiae* individuals. *An. arabiensis* were assigned to the orange population with the highest probabilities, separating them from all *An. gambiae* mosquitoes. The island *An. gambiae* were mostly assigned to the

blue but with slightly more uncertainly. Much of the variation was recorded between populations (*An. gambiae* island and mainland individuals and *An. arabiensis* individuals) instead of among individuals within a site. These results from STRUCTURE (Figure 6B) were also largely consistent with those from PCA (Figure 5A-C) with clear separation at an interspecific level and no clear separation at the intraspecific level.

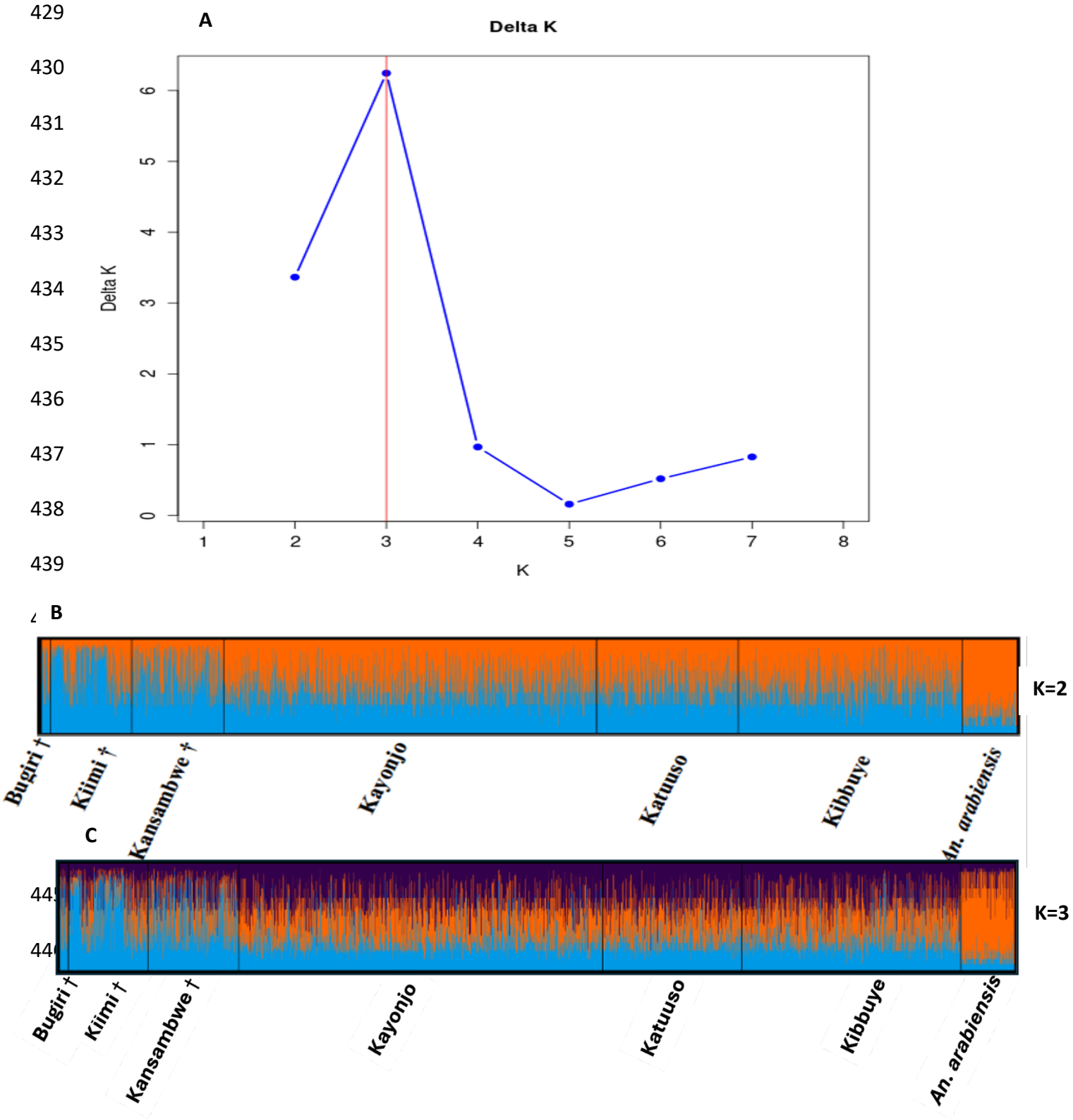

448 **Figure 6:** Outputs from Bayesian clustering analysis for the 2918 *An. gambiae* and 173 *An.*
449 *arabiensis*. **(A)** The optimal number of clusters (*K=3*) based on the Evanno et al [61] method
450 showing deltaK **(B)** Bar plot representing K=2 of 3091 mosquitoes, each represented by a thin
451 vertical bar colored in proportion to their estimated ancestry within each cluster (**C**) Bar plot
452 representing K=3 of 3091 mosquitoes. A vertical black line bounds each site and the labels
453 with † for islands while those without are for mainland samples.

454 **Genetic diversity and neutrality tests**

455 Nucleotide diversity (π) and Tajima's D were calculated for each *An. gambiae* population (SI
456 Table S1), then further for each chromosome arm (Figure 7A). The overall nucleotide diversity
457 for *An. gambiae* was 0.0115 (range from 0.0107 to 0.01169, SI Table S1) and that of *An.*
458 *arabiensis* was 0.00859 (ranging from 0.00829 to 0.00859; SI Table 2). Generally, higher
459 diversity values were reported for mainland *An. gambiae* populations (0.01143 to 0.01169; SI
460 Table 1) compared to those for island sites (0.01071 to 0.01103; SI Table 1). On the other hand,
461 the diversity values for *An. arabiensis* mainland populations were lower compared to the
462 mainland *An. gambiae* populations. The pattern of nucleotide diversity compared between
463 chromosomes for different sites (Figure 7B) was consistent across all sites and chromosome
464 arms (mainland sites' p > island sites' p). At each site, mean chromosomal nucleotide diversity
465 was highest on the 3R chromosome and lowest on the 2R arm. However, pooled *An. arabiensis*
466 (from all locations) had an overall low diversity compared to the different *An. gambiae*
467 populations, with the lowest diversity in the 2R chromosome arm (P = 0.031, Figure 7B).
468 Overall, the pooled island and mainland diversity falls between the values for each sample site
469 across chromosome arms (Figure 7B).

Mean Tajima's D was negative for all sites, an indication of an excess of rare alleles and thus a deviation from the neutral model of a well-mixed population of constant size. However, unlike the *An. gambiae* mainland populations, Tajima's D values for *An. gambiae* island sites and all *An. arabiensis* populations were not statistically significant from from zero (SI Table S1, S2). When tested for each chromosome and site, all Tajima's D values were negative. The same was done for the *An. arabiensis* mainland populations (SI Table S2). The Tajima's D value of the pooled *An. arabiensis* chromosome 2R arm was significantly more negative than other arms of the same site (P = 0.031), and the 2R arm of the individual and pooled populations.

A

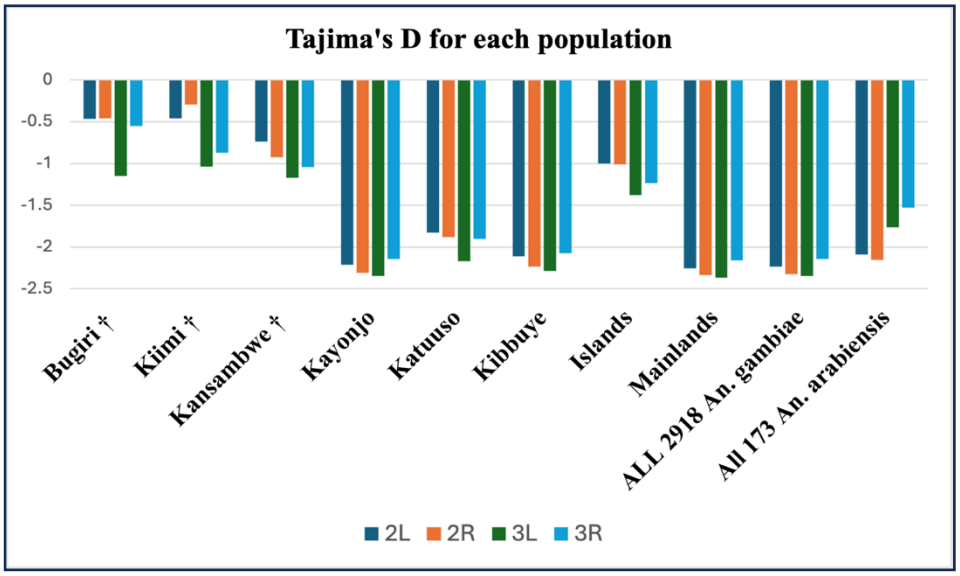

B

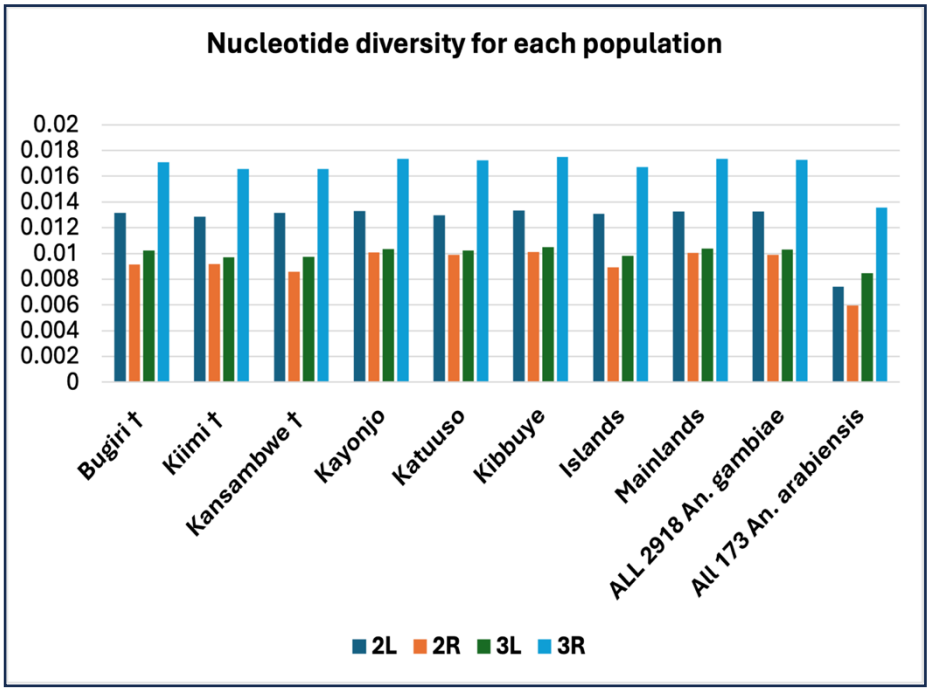

Figure 7: (A) Tajima's D for the six *An. gambiae* populations per chromosome arm. In addition, we calculated the same statistic for the following subsets: pooled *An. gambiae* from the island and the mainland sites, then all *An. gambiae*, and all *An. arabiensis* (**B)** Nucleotide diversity (π) for the six *An. gambiae* populations per chromosome arm. † Denotes an island site.

Contemporary effective population size (*Ne*)

Generally, for *An. gambiae* populations, smaller Ne values were observed for the island sites (between 146 and 249), compared to mainland sites (between 4054 and 8190) (Table 4A). The point estimate for Bugiri was inconclusive but came with a very small lower bound. For the *An. arabiensis* populations, we only estimated Ne for the mainland sites, and their estimates were comparable to the mainland *An. gambiae* populations. (Table 4B).

517 **Table 4: Contemporary Ne estimates**

518 **A. *An. gambiae***

Site	No. of individuals	Number of sites	Overall r^2	Estimated Ne
Bugiri†	28	37	0.035383	∞ (15.1 – ∞)
Kiimi†	258	32	0.006168	146.4 (61.7–640.2)
Kansambwe†	294	32	0.004764	249.3 (146.7– 538.5)
Kayonjo	1178	15	0.000901	6723.1 (515.9 - ∞)
Katuuso	450	27	0.002181	4054.1 (640.9 - ∞)
Kibbuye	710	21	0.001416	8190.9 (521.5 - ∞)

519

520 ***B.* An*. arabiensis***

Site	No. of individuals	Number of sites	Overall r^2	Estimated Ne
Kayonjo	51	31	0.018910	∞ (49.4- ∞)
Katuuso	39	35	0.027836	3402.8 (36.3 - ∞)
Kibbuye	78	31	0.013438	3587.4 (95.9 – ∞)

521 Site choice is described in the main text. † Denotes island sites. 0.01 was the lowest allele

522 frequency used. The values in parentheses represent the jackknife range.

523

524

525

526

527

528 **Discussion**

529 **Polymorphic sites and population structure**

530 From the 62 amplicon loci, 9890 sites were mapped onto the reference genome, many of
531 which were fixed sites (Figure 3) or weakly polymorphic due to the conserved nature of the
532 primer-binding regions (Figure 2). Despite this limitation, the data revealed useful insights into
533 the population structure of *An. gambiae* and *An. arabiensis* in Uganda. Overall, genetic
534 differentiation among the *An. gambiae* populations was generally low regardless of the sites
535 ($F_{ST} < 0.05$), though statistically significant in some cases, suggesting subtle structure with
536 ongoing connectivity.

537 The high gene flow observed between Bugiri (island) and other sites could be influenced by
538 several factors. One potential cause is human-mediated transport, as frequent boat traffic and
539 ferries between Bugiri and other sites can inadvertently facilitate mosquito dispersal [62–64].
540 Additionally, prevailing seasonal wind and weather patterns might assist mosquito flight over
541 water, enhancing connectivity [65,66]. These mechanisms together contribute to the low
542 genetic differentiation reported for Bugiri compared to other island populations. However, the
543 low F_{ST} value observed for Bugiri could also be influenced by its relatively small sample size ,
544 which can increase sampling variance and reduce the power to detect subtle genetic
545 differentiation [67,68].

546 In contrast, *An. arabiensis* mainland populations exhibited very low and often negative F_{ST}
547 values, consistent with unrestricted gene flow [46,69,70]. The negative F_{ST} values (between
548 Katuuso and Kibbuye) likely reflects greater within-site genetic diversity than between-sites
549 genetic diversity, indicative of stable and large Ne [71,72].

550 One notable feature of our results is the presence of low but statistically significant F_{ST} values
551 among many population pairs, indicating that while the genetic differentiation is subtle,
552 structure nonetheless exists. F_{ST} values for island *An. gambiae* species were however higher
553 compared to mainland sites, reflecting restricted gene flow across water barriers, smaller
554 population sizes, and potential local adaptation comparable to what was reported in previous
555 studies [26,27,34]. This could be justified by the large mainland population, given that F_{ST} is
556 approximately $1/1 + 4Nm$, where N is the effective population size and m the migration rate
557 [72]. Thus, using our estimated large mainland populations for N, the low F_{ST} values between
558 sites equate to substantial numbers of migrants per generation, reinforcing connectivity
559 among sites [68,72]. Given that these F_{ST} values are significantly greater than zero
560 demonstrates that the populations are not panmictic or identical but exhibit genuine
561 population structure [73,74]. Recognizing this subtle but meaningful structure is crucial when
562 considering the design and spread dynamics of gene drive or insecticide resistance alleles.

563 Looking at this from a malaria vector control perspective, high gene flow is a double edged
564 sword. On one hand, it promotes the spread of gene drive constructs throughout connected
565 mosquito populations, potentially enabling rapid spread of desired genetic traits [75].
566 Conversely, it complicates containment, given that, genetic modifications could
567 unintentionally spread beyond target areas, raising ecological and regulatory concerns.
568 Moreover, convergent evolution may promote the rise of resistance alleles that impair gene
569 drive function, necessitating careful monitoring [76].

570 It is thus important to distinguish between whether low differentiation results are from
571 ongoing gene flow, convergent adaptation, or both, and understanding these dynamics allows

572 for better-informed strategies to optimize gene drive deployment, balancing efficacy with
573 biosafety in malaria vector control.

574 Low point estimates of pairwise fst yielded high Z_scores, suggesting the presence of subtle
575 yet statistically significant population structure despite low apparent differentiation. This
576 occurrence can largely be attributed to the statistical power afforded by a large sample size,
577 which can detect even minor genetic differences across sites [77,78]. Between Kiimi and
578 Katuuso, the low pairwise fst value and non-significant P-value could be because of temporal
579 sampling variability, which could result in capturing different allele frequencies due to
580 temporal fluctuations [79–81]. These comparisons of the relative amounts of gene flow taking
581 place between sites, aid in predicting the trajectory of the alleles introduced by gene drive
582 into the wild-type population [21].

583 The Mantel test results (P=0.052) suggested only weak evidence of isolation by distance [82],
584 suggesting that geographic distance partly influences gene flow, which could thus be factored
585 into spatially targeted vector control interventions [68]. Therefore, according to the IBD
586 hypothesis, there may be a meaningful association between the genetic and geographical
587 distances among populations. Therefore, tailored intervention deployment considering spatial
588 genetic structure can optimise control effectiveness.

589 PCA distinguished species but did not reveal clear geographical structure within *An. gambiae*.
590 These findings align with doubleton analysis (Table 3), which highlighted relative isolation of
591 island sites and stronger connectivity at mainland sites.

592 The moderate within-group isolation of the *arabiensis* group (Table 3) indicates more frequent
593 genetic interactions within this group than expected, potentially due to localized genetic

594 structures, ecological factors, or other selective pressures driving allele frequencies. This could
595 reflect a localized population structure which may arise from ecological factors like
596 microhabitat variation, behavioural differences or localized selective pressures, that can
597 restrict gene flow at finer spatial scales despite the species' wide distribution.

598 The counts between *arabiensis* and *mainland_gam* groups indicate a degree of gene flow,
599 implying occasional genetic exchange, which could have direct implications for vector control,
600 especially given the differential patterns of gene flow and inbreeding detected across these
601 sites. This pattern of observed versus expected doubleton pairs sides with the broader view
602 of population structure in malaria vectors, where poor gene flow across ecological boundaries
603 frequently results in discrete genetic clusters [83], and has implications on both gene drive
604 strategies and management of insecticide resistance.

605 STRUCTURE analysis identified three major clusters (Figure 6) corresponding to species and
606 geography, consistent with F_{ST} and PCA results. STRUCTURE results reflect what is often
607 observed when there is low genetic differentiation [84]. STRUCTURE output for the *An.*
608 *gambiae* and *An. arabiensis* species at each site showed sharing of ancestry between each
609 individual at differing proportions (with differing consistency between all island, mainland *An.*
610 *gambiae* and *An. arabiensis* individuals). The three genetic clusters corresponded to first
611 species (*An. arabiensis*) then to geographical (mainland and island *An. gambiae*) differences,
612 with relatively more similarity between island compared to mainland *An. gambiae* individuals
613 (Figure 6B). These results are comparable to the F_{ST} and PCA results that show less divergence
614 between island and mainland *An. gambiae* individuals and more diversity (clear separation)
615 between *An. gambiae* and *An. arabiensis* individuals [55,56].

616 Despite using very few polymorphic sites, STRUCTURE was able to outline the three clusters
617 with visible differences. Therefore, using more sites could produce clearer and more distinct
618 clustering. And because pairwise F_{ST} is sensitive to allele frequency differences between sites
619 and works best when populations are distinct and genetically isolated, it may not always
620 capture subtle population differentiation, while STRUCTURE, on the other hand, assigns
621 individuals to clusters based on their multilocus genotypes, and is thus more sensitive to
622 subtle population differentiation [44,73,85,86].

623 **Genetic diversity and neutrality tests**

624 Negative Tajima's D values (SI Tables S1&S2), especially at mainland sites, suggested an excess
625 of low frequency alleles, potentially reflecting recent population expansion or purifying
626 selection [87–89]. These results were in line with previous findings [83]. Given that *An*.
627 *gambiae* thrives in human dorminated environments, its population and range will thus
628 expand most in areas where human population density is high and growing, whether on island
629 or mainland sites [90].

630 The observed differences in Tajima's D and nucleotide diversity between island and mainland
631 *An. gambiae* populations provide further evidence that these are distinct populations rather
632 than a single panmictic unit. Mainland populations exhibited significantly higher nucleotide
633 diversity and more negative Tajima's D values, consistent with recent population expansion
634 and larger effective population sizes [72,91]. In contrast, island populations showed
635 marginally lower nucleotide diversity and Tajima's D values not significantly different from
636 zero (SI Table S1, S2), suggesting small but stable effective population sizes or mutation-drift
637 equilibrium, with no population bottleneck or expansion, an occurrence consistent with the
638 neutral mutation hypothesis [92,93]. These genetic differences, together with the subtle but

639 significant population structure detected by F_{ST} and clustering analyses, support the
640 conclusion that island and mainland *An. gambiae* populations are genetically differentiated
641 and should be considered as separate population units for vector control considerations
642 [34,64].

643 These estimates were within the range of values reported in previous studies which utilised
644 four loci (white, tox, G6pd, xdh) across several African locations [94] and immune-related
645 (LRIM1, CTL4, CTLMA2, APL2) and housekeeping genes [95], and were consistent with the fact
646 that populations at island sites display marginally lower nucleotide diversity compared to the
647 mainland [96,97]. The explanation for this could be inbreeding, or higher degree of isolation
648 with small neighborhood size [96,98–100].

649 On the 2R chromosome arm, the pooled *An. arabiensis* population has lower nucleotide
650 diversity than individual or pooled *An. gambiae* populations, which could be because the 2R
651 arm has many segregating inversions, some of which are polymorphic in *An. gambiae* and
652 fixed in *An. arabiensis,* which inversions can limit recombination in certain regions, leading to
653 reduced genetic diversity over time [101,102]. This phenomenon is especially pronounced in
654 species like *An. arabiensis*, where these inversions (2La, 2Rb and 3Ra) could be fixed, and
655 further decrease genetic variation along the 2R chromosome relative to *An. gambiae*
656 populations [103,104].

657 Additionally, the frequencies for inversions segregating in both species could be/are different
658 for the two species [102], suggesting a decline in population size and/or balancing selection,
659 a feature of the maintenance of segregating 2Rb, c, d, u and j inversions [90,105].

660

661 **Contemporary effective population size**

662 Ne estimates were smaller for island *An. gambiae* than at mainlands sites, reflecting isolation
663 and stronger drift, results comparable to those reported in the Kayondo et al. and Wiltshire et
664 al. studies [28–30]. The low Ne estimates at island sites could be because of their small
665 neighbourhood size and are suggestive of higher levels of genetic differentiation (presented
666 as pairwise F_{ST} estimates) shown in Table 4A [59].

667 Mosquito populations at these smaller, more isolated sites are more vulnerable to genetic drift,
668 but may also be more amenable to localized control interventions.

669 The infinity values of point estimates such as those recorded for Bugiri, was almost certainly
670 due to insufficient sample size compared to the magnitude of genetic drift. The infinite
671 jackknife upper bound at the mainland sites suggests that based on the LD observed, it's
672 statistically feasible that Ne could be extremely large, although the exact size cannot be
673 pinpointed with certainty [106–108].

674 Larger Ne in the mainland *An. gambiae* populations suggest higher resilience to vector control
675 interventions and more likely to sustain the spread of resistance alleles [109–113]. This implies
676 slower genetic drift which allows for sustained genetic variation that enhances adaptation to
677 environmental changes, and because dry season surviving populations can rebound and
678 maintain genetic diversity across seasons, this further complicates efforts to control malaria
679 vector populations [114–118].

680 **Implications for malaria vector control**

681 These findings have important implications for: (1) insecticide resistance: high connectivity
682 among mosquitoes at mainland sites facilitate rapid spread of resistance alleles, where as

island isolation may slow spread and allow for localised resistance management, (2) Gene drive strategies: the reduced Ne and relative isolation of mosquitoes at island sites lower the release threshold for gene drives, increasing the likelihood of successful establishment [21]. Relative isolation and smaller Ne values favours islands as contained experimental sites for gene drive trials, allowing more manageable monitoring and containment [75]. Conversely, large, well-connected mainland sites would require larger releases and careful management to ensure effective drive propagation, and (3) Vector elimination efforts: The weak but detectable structure among *An. gambiae* populations suggests that control efforts need to account for ongoing gene flow between sites. Local elimination on islands may be feasible, but reinvasion from the mainland remains a threat.

The ease of access to the islands (which allows easy monitoring), higher genetic differentiation, genetic structure, smaller effective population sizes compared to mainland sites, and their small geographical size, makes islands ~~are~~ promising sites for field trials to test the effectiveness of mosquito gene drive systems.

And as mentioned at the start, *An. arabiensis* individuals are often excluded from further analysis due to their limited numbers in the mosquito collections done to date [26,27,34], which could be because of the sampling methods used. Therefore, studies that target the exophilic and zoophagic characteristics of this species should be carried out to give a better picture of its density, specifically at the islands which are the potential sites for field trials to test mosquito gene drive systems. This will help us to confirm the proportion of the non-target malaria vector species at the island sites.

As much as we would like to provide a comprehensive perspective of the overall spatial and temporal variation of the two species in Uganda, the latter cannot be investigated here

706 because of the different sampling times in the island and mainland sampling. We welcome
707 further studies on other biological factors, such as the mosquitoes' seasonal dynamics and
708 dry season persistence mechanisms [119,120], as these may contribute to the observed
709 population structure.

710 Future works should include a dataset using whole genome sequenced data, exploring
711 temporal sampling, further investigations into the specific contribution of the suggested
712 factors we have used, as well as the influence of other suggested biotic (e.g., passive
713 transport) and abiotic factors (e.g., seasonality and chromosome inversions) that may
714 contribute to the observed differentiation. These will add a valuable body of information
715 required for evaluating these Islands as potential release sites for mosquito gene drive
716 systems.

717 **Conclusion**

718 Despite limited polymorphism in the loci studied, this work highlights subtle but meaningful
719 population structure between *An. gambiae* and *An. arabiensis* populations. The contrast
720 between small, isolated island sites and large, connected mainland sites has direct
721 consequences for the design of insecticide resistance management strategies, feasibility of
722 gene drive interventions, and broader malaria vector control approaches.

723

724

725

726

727

728

Acknowledgements

We are grateful to Cindy Sewon, a former undergraduate student at Imperial College, London for her valuable contributions, John B. Connolly, Silke Fuchs and Samantha O'Loughlin for their support and helpful comments towards this work, and the field team that did the mosquito sample collection.

Conflict of interest

The authors declare no conflicts of interest. The funding bodies had do direct role in the design of the study nor in the collection, analysis, interpretation of data or in the writing of the manuscript

Author contributions

JK conceived the research topic, hosted lab and field work. ML hosted the targeted amplicon sequencing. MB and AM participated in amplicon sequencing. EL supported in bioinformatics processing. RM and TH analysed the data. RM wrote the manscript with inputs from all other authors. All authors read and approved the final manuscript.

Funding

This work was supported by the Bill & Melinda Gates Foundation and the Open Philanthropy Project, an advised fund of the Silicon Valley Community Foundation.

References

1. Bhatt S, Weiss DJ, Cameron E, Bisanzio D, Mappin B, Dalrymple U, et al. The effect of malaria control on Plasmodium falciparum in Africa between 2000 and 2015. 2015;526:207–11.
2. Lehmann T, Dao A, Yaro AS, Adamou A, Kassogue Y, Diallo M, et al. Aestivation of the African Malaria Mosquito, Anopheles gambiae in the Sahel. American Journal of Tropical Medicine & Hygiene. 2010;83:601–6.
3. WHO. World Malaria Report. World Health Organization; 2024.
4. WHO. World Malaria Report. World Health Organization. 2023.
5. WHO. World Malaria Report. World Health Organization. 2022.
6. Hemingway J. The role of vector control in stopping the transmission of malaria: Threats and opportunities. Philosophical Transactions of the Royal Society B: Biological Sciences. Royal Society; 2014.
7. Mushtaq I, Sarwar MS, Chaudhry A, Shah SAH, Ahmad MM. Updates on traditional methods for combating malaria and emerging Wolbachia-based interventions. Front Cell Infect Microbiol. Frontiers Media SA; 2024.
8. Plowe C V. Malaria chemoprevention and drug resistance: a review of the literature and policy implications. Malar J. BioMed Central Ltd; 2022.
9. Thu AM, Phyo AP, Landier J, Parker DM, Nosten FH. Combating multidrug-resistant Plasmodium falciparum malaria. FEBS Journal. Blackwell Publishing Ltd; 2017. p. 2569–78.
10. Kaddumukasa MA, Wright J, Muleba M, Stevenson JC, Norris DE, Coetzee M. Genetic differentiation and population structure of Anopheles funestus from Uganda and the southern African countries of Malawi, Mozambique, Zambia and Zimbabwe. Parasit Vectors [Internet]. 2020;13:1–13. Available from: https://doi.org/10.1186/s13071-020-3962-1
11. Hammond A, Pollegioni P, Persampieri T, North A, Minuz R, Trusso A, et al. Gene-drive suppression of mosquito populations in large cages as a bridge between lab and field. Nat Commun. 2021;12.
12. Marshall JM, Akbari OS. Gene Drive Strategies for Population Replacement. Genetic Control of Malaria and Dengue. 2016;169–200.
13. Burt A. Heritable strategies for controlling insect vectors of disease. Philosophical Transactions of the Royal Society B: Biological Sciences. 2014;369.
14. Gantz VM, Jasinskiene N, Tatarenkova O, Fazekas A, Macias VM, Bier E, et al. Highly efficient Cas9-mediated gene drive for population modification of the malaria vector mosquito *Anopheles stephensi*. Proc Natl Acad Sci U S A. 2015;112:E6736–43.
15. Hammond MA, Galizi R. Gene drives to fight malaria: current state and future directions. Pathog Glob Health. 2017;111:412–23.
16. Makunin A, Korlević P, Park N, Goodwin S, Waterhouse RM, von Wyschetzki K, et al. A targeted amplicon sequencing panel to simultaneously identify mosquito species and Plasmodium presence across the entire *Anopheles* genus. Mol Ecol Resour. 2022;22:28–44.
17. Galizi R, Doyle LA, Menichelli M, Bernardini F, Deredec A, Burt A, et al. A synthetic sex ratio distortion system for the control of the human malaria mosquito. Nat Commun. 2014;5.
18. Gantz VM, Bier E. The mutagenic chain reaction: A method for converting heterozygous to homozygous mutations. Science (1979). 2015;348:442–4.

19. Hammond A, Galizi R, Kyrou K, Simoni A, Siniscalchi C, Katsanos D, et al. A CRISPR-Cas9 gene drive system targeting female reproduction in the malaria mosquito vector *Anopheles gambiae*. Nat Biotechnol. 2016;34:78–83.
20. Ng'habi, R., K., Knols, J., G., B., Lee, Y., Ferguson, M., H. and Lanzaro, C. G. Population genetic structure of Anopheles arabiensis and Anopheles gambiae in a malaria endemic region of southern Tanzania. Malar J. 2011;10.
21. Lanzaro GC, Tripet F. Gene flow among populations of *Anopheles gambiae*: a critical review. 2003;1–24. Available from: http://edepot.wur.nl/136907%5Cnpapers3://publication/uuid/F232B8BC-F74F-456E-A0DB-11E8198EE5B1
22. Lanzaro GC, Touré YT, Carnahan J, Zheng L, Dolo G, Traoré S, et al. Complexities in the genetic structure of *Anopheles gambiae* populations in west Africa as revealed by microsatellite DNA analysis. Proc Natl Acad Sci U S A. 1998;95:14260–5.
23. Burt A. Site-specific selfish genes as tools for the control and genetic engineering of natural populations. Proceedings of the Royal Society B: Biological Sciences. 2003;270:921–8.
24. Naidoo K, Oliver S V. Gene drives: an alternative approach to malaria control? Gene Ther. Springer Nature; 2024.
25. Hancock PA, North A, Leach AW, Winskill P, Ghani AC, Godfray HCJ, et al. The potential of gene drives in malaria vector species to control malaria in African environments. Nat Commun [Internet]. 2024;15:8976. Available from: https://www.nature.com/articles/s41467-024-53065-z
26. Wiltshire MR, Bergey MC, Kayondo KJ, Birungi J, Mukwaya GL, Emrich JS, et al. Reduced-representation sequencing identifies small effective population sizes of *Anopheles gambiae* in the north-western Lake Victoria basin, Uganda. Malar J. 2018;17.
27. Kayondo, K., J., Mukwaya, G., L., Stump, A., Michel, P., A., Coulibaly, B., M., Besansky, J., N. and Collins, H. F. Genetic structure of Anopheles gambiae populations on islands in northwestern Lake Victoria, Uganda. Malar J. 2005;4.
28. Kayondo, K., J., Mukwaya, G., L., Stump, A., Michel, P., A., Coulibaly, B., M., Besansky, J., N. and Collins, H. F. Genetic structure of Anopheles gambiae populations on islands in northwestern Lake Victoria, Uganda. Malar J. 2005;4.
29. Lukindu, M., Bergey, M., C., Wiltshire, M., R., Small, T., S., Bourke, P., B., Kayondo, K., J. and Besansky, J. N. Spatio-temporal genetic structure of Anopheles gambiae in the Northwestern Lake Victoria Basin, Uganda: implications for genetic control trials in malaria endemic regions. Parasit Vectors. 2018;11.
30. Wiltshire, M., R., Bergey, M., C., Kayondo, K., J. et al. Reduced-representation sequencing identifies small effective population sizes of Anopheles gambiae in the north-western Lake Victoria basin, Uganda. Malar J. 2018;17.
31. M. DJ, Cuamba N., Charlwood JD, F. CH, Townson H. Population structure in the malaria vector, Anopheles arabiensis Patton, in East Africa. Heredity (Edinb). 1999;83:408–17.
32. Della Torre A, Tu Z, Petrarca V. On the distribution and genetic differentiation of *Anopheles gambiae s.s.* molecular forms. Insect Biochem Mol Biol. 2005;35:755–69.
33. O'Loughlin SM, Magesa S, Mbogo C, Mosha F, Midega J, Lomas S, et al. Genomic analyses of three malaria vectors reveals extensive shared polymorphism but contrasting population histories. Mol Biol Evol. 2014;31:889–902.
34. Lukindu M, Bergey MC, Wiltshire MR, Small TS, Bourke PB, Kayondo KJ, et al. Spatio-temporal genetic structure of *Anopheles gambiae* in the Northwestern Lake Victoria Basin,

Uganda: implications for genetic control trials in malaria endemic regions. Parasit Vectors. 2018;11.
35. Okech BA, Gouagna LC, Killeen GF, Knols BGJ, Kabiru EW, Beier JC, et al. Influence of sugar availability and indoor microclimate on survival of *Anopheles gambiae* (Diptera: Culicidae) under semifield conditions in western Kenya. J Med Entomol. 2003;40:657–63.
36. Ngowo HS, Kaindoa EW, Matthiopoulos J, Ferguson HM, Okumu FO. Variations in household microclimate affect outdoor-biting behaviour of malaria vectors [version 1; referees: 2 approved, 1 approved with reservations]. Wellcome Open Res. 2017;2:1–18.
37. Zhong D, Wang X, Xu T, Zhou G, Wang Y, Lee MC, et al. Effects of microclimate condition changes due to land use and land cover changes on the survivorship of malaria vectors in China-Myanmar border region. PLoS One. 2016;11.
38. Gillies MT, and, Coetzee M. A supplement to the *Anopheline* of Africa South of the Sahara (Afro-Tropical region). South African Institute for Medical Research. 1987;55.
39. Boddé M, Makunin A, Ayala D, Bouafou L, Diabaté A, Ekpo UF, et al. High-resolution species assignment of *Anopheles* mosquitoes using k-mer distances on targeted sequences. Elife. 2022;11:1–40.
40. Kingma DP, Welling M. Auto-Encoding Variational Bayes. 2013; Available from: http://arxiv.org/abs/1312.6114
41. Nagi SC, Lucas ER, Ashraf F, Mugoya T, Lukyamuzi E, Summers S, et al. Targeted genomic surveillance of insecticide resistance in African malaria vectors [Internet]. 2025. Available from: http://biorxiv.org/lookup/doi/10.1101/2025.02.14.637727
42. Ochoa A, Storey JD. FST and kinship for arbitrary population structures I: Generalized definitions [Internet]. 2016. Available from: http://biorxiv.org/lookup/doi/10.1101/083915
43. Ochoa A, Storey JD. Estimating FST and kinship for arbitrary population structures. PLoS Genet. 2021;17.
44. Pritchard KJ, Stephens M, Donnelly P. Inference of Population Structure Using Multilocus Genotype Data. Genetics. 2000;155:945–959.
45. Ochola A. SJD. popkinsuppl: supplement to popkin package [Internet]. 2022. Available from: https://github.com/OchoaLab/popkinsuppl.
46. Bhatia G, Patterson N, Sankararaman S, Price AL. Estimating and interpreting F ST : The impact of rare variants. Genome Res. 2013;23:1514–21.
47. Arnold B, Corbett-Detig RB, Hartl D, Bomblies K. RADseq underestimates diversity and introduces genealogical biases due to nonrandom haplotype sampling. Mol Ecol. 2013;22:3179–90.
48. Efron B, Tibshirani JR. An introduction to the Bootstrap. Cox DR, Hinkley D V, Reid N, Rubin DB, Silverman BW, editors. Regression Analysis with Applications B.G. Wetherill. Taylor & Francis Group; 1994.
49. Peakall R, Smouse PE. GenALEx 6.5: Genetic analysis in Excel. Population genetic software for teaching and research-an update. Bioinformatics. 2012;28:2537–9.
50. Diniz-Filho JAF, Soares TN, Lima JS, Dobrovolski R, Landeiro VL, Telles MP de C, et al. Mantel test in population genetics. Genet Mol Biol. 2013;36:475–85.
51. Patterson N, Price AL, Reich D. Population Structure and Eigenanalysis. PLoS Genet. 2006;2.
52. Team RC. R: A language and environment for statistical computing. R Foundation for statistical computing, Vienna, Austria. 2023.
53. Evanno G, Regnaut S, Goudet J. Detecting the number of clusters of individuals using the software STRUCTURE: A simulation study. Mol Ecol. 2005;14:2611–20.

54. Kopelman NM, Mayzel J, Jakobsson M, Rosenberg NA, Mayrose I. Clumpak: A program for identifying clustering modes and packaging population structure inferences across K. Mol Ecol Resour. 2015;15:1179–91.
55. Nei M, Miller JC. A simple method for estimating average number of nucleotide substitutions within and between populations from restriction data. Genetics. 1990;125:873–9.
56. Tajima F. Statistical Method for Testing the Neutral Mutation Hypothesis by DNA Polymorphism. Genetics Society of America. 1989;123:585–95.
57. Paradis E. Pegas: An R package for population genetics with an integrated-modular approach. Bioinformatics. 2010;26:419–20.
58. Waples, S. , R. & Do C. LDNE: a program for estimating effective population size from data on linkage disequilibrium. Mol Ecol Resour. 2008;8:753–6.
59. Do C, Waples RS, Peel D, Macbeth GM, Tillett BJ, Ovenden JR. NeEstimator v2: Re-implementation of software for the estimation of contemporary effective population size (Ne) from genetic data. Mol Ecol Resour. 2014;14:209–14.
60. F. R. Genetic Differentiation and Estimation of Gene Flow from FStatistics Under Isolation by Distance. Genetics. 1997;34:399–405.
61. Evanno G, Regnaut S, Goudet J. Detecting the number of clusters of individuals using the software STRUCTURE: A simulation study. Mol Ecol. 2005;14:2611–20.
62. Service MW. Mosquito (Diptera: Culicidae) Dispersal-The Long and Short of It. J Med Entomol [Internet]. 1997;34:579–88. Available from: https://academic.oup.com/jme/article/34/6/579/2221644
63. Bataille A, Cunningham AA, Cruz M, Cedeño V, Goodman SJ. Adaptation, isolation by distance and human-mediated transport determine patterns of gene flow among populations of the disease vector Aedes taeniorhynchus in the Galapagos Islands. Infection, Genetics and Evolution. 2011;11:1996–2003.
64. Kayondo JK, Mukwaya LG, Stump A, Michel AP, Coulibaly MB, Besansky NJ, et al. Genetic structure of *Anopheles gambiae* populations on islands in northwestern Lake Victoria, Uganda. Malar J. 2005;4.
65. Atieli HE, Zhou G, Zhong D, Wang X, Lee MC, Yaro AS, et al. Wind-assisted high-altitude dispersal of mosquitoes and other insects in East Africa. J Med Entomol. 2023;60:698–707.
66. Sanogo ZL, Yaro AS, Dao A, Diallo M, Yossi O, Samaké D, et al. The effects of high-altitude windborne migration on survival, oviposition, and blood-feeding of the african malaria mosquito, *Anopheles gambiae s.l.* (Diptera: Culicidae). J Med Entomol. 2021;58:343–9.
67. Kalinowski ST. Do polymorphic loci require large sample sizes to estimate genetic distances? Heredity (Edinb). 2005;94:33–6.
68. Slatkin M. Gene Flow and the Geographic Structure of Natural Populations [Internet]. 1987. Available from: https://www.science.org
69. Charlesworth B. Measures of Divergence Between Populations and the Effect of Forces that Reduce Variability. Mol Biol Evol [Internet]. 1998;15:538–43. Available from: https://academic.oup.com/mbe/article/15/5/538/987854
70. Hudson RR, Slatkint M, Maddison WP. Estimation of Levels of Gene Flow From DNA Sequence Data. 1992.
71. Smaragdov MG, Kudinov AA, Uimari P. Assessing the genetic differentiation of holstein cattle herds in the Leningrad region using Fst statistics. Agricultural and Food Science. 2018;27:96–101.

72. Hartl DL, Clark AG. PRINCIPLES OF POPULATION GENETICS. 4th ed. Sinauer Associates; 2007.
73. Holsinger KE, Weir BS. Genetics in geographically structured populations: Defining, estimating and interpreting FST. Nat Rev Genet. 2009. p. 639–50.
74. Wright S. The genetical structure of populations. nnals of Eugenics. 1951;15:323–354.
75. North AR, Burt A, Godfray HCJ, North, R., A., Burt, A. and Godfray, J., H. C. Modelling the potential of genetic control of malaria mosquitoes at national scale. BMC Biol. 2019;17:1–12.
76. Unckless RL, Clark AG, Messer PW. Evolution of resistance against CRISPR/Cas9 gene drive. Genetics. 2017;205:827–41.
77. Das S, Máquina M, Phillips K, Cuamba N, Marrenjo D, Saúte F, et al. Fine-scale spatial distribution of deltamethrin resistance and population structure of *Anopheles funestus* and *Anopheles arabiensis* populations in Southern Mozambique. Malar J. 2023;22.
78. Fumagalli M. Assessing the effect of sequencing depth and sample size in population genetics inferences. PLoS One. 2013;8.
79. Bi K, Linderoth T, Singhal S, Vanderpool D, Patton JL, Nielsen R, et al. Temporal genomic contrasts reveal rapid evolutionary responses in an alpine mammal during recent climate change. PLoS Genet. 2019;15.
80. Machado HE, Bergland AO, Taylor R, Tilk S, Behrman E, Dyer K, et al. Broad geographic sampling reveals the shared basis and environmental correlates of seasonal adaptation in drosophila. Elife. 2021;10.
81. Sandoval-Castellanos E. Testing temporal changes in allele frequencies: A simulation approach. Genet Res (Camb). 2010;92:309–20.
82. Diniz-Filho JAF, Soares TN, Lima JS, Dobrovolski R, Landeiro VL, Telles MP de C, et al. Mantel test in population genetics. Genet Mol Biol. 2013;36:475–85.
83. The Anopheles gambiae 1000 Genomes consortium. Genetic diversity of the African malaria vector Anopheles gambiae. Nature. 2017;552:96–100.
84. Guillot G. Inference of structure in subdivided populations at low levels of genetic differentiation - The correlated allele frequencies model revisited. Bioinformatics. 2008;24:2222–8.
85. Weir BS, Cockerham CC. Estimating F-statistics for the analysis of population structure. Evolution (N Y). 1984;38:1358–70.
86. Jombart T, Devillard S, Balloux F. Discriminant analysis of principal components: A new method for the analysis of genetically structured populations. BMC Genet. 2010;11.
87. Nielsen R. Molecular signatures of natural selection. Annu Rev Genet. 2005. p. 197–218.
88. Kreitman M. Methods to detect selection in populations with applications to the human. Annu Rev Genomics Hum Genet. 2000;1:539–59.
89. Tajima F. Statistical Method for Testing the Neutral Mutation Hypothesis by DNA Polymorphism. 1989.
90. O'Loughlin SM, Magesa S, Mbogo C, Mosha F, Midega J, Lomas S, et al. Genomic analyses of three malaria vectors reveals extensive shared polymorphism but contrasting population histories. Mol Biol Evol. 2014;31:889–902.
91. Nei M, Li WH. Mathematical model for studying genetic variation in terms of restriction endonucleases. Proc Natl Acad Sci U S A. 1979;76:5269–73.
92. Parimittr P, Chareonviriyaphap T, Bangs MJ, Arunyawat U. Genetic variation of Aedes aegypti mosquitoes across Thailand based on nuclear DNA sequences. Agriculture and Natural Resources. 2018;52:596–602.

93. Dharmarathne HAKM, Weerasena OVDSJ, Perera KLNS, Galhena G. Genetic characterization of Aedes aegypti (Diptera: Culicidae) in Sri Lanka based on COI gene. J Vector Borne Dis. 2020;57:153–60.
94. Besansky NJ, Krzywinski J, Lehmann T, Simard F, Kernt M, Mukabayire O, et al. Semipermeable species boundaries between *Anopheles gambiae* and *Anopheles arabiensis*: Evidence from multilocus DNA sequence variation. Proc Natl Acad Sci U S A. 2003;100:10818–23.
95. Obbard DJ, Linton YM, Jiggins FM, Yan G, Little TJ. Population genetics of Plasmodium resistance genes in *Anopheles gambiae*: No evidence for strong selection. Mol Ecol. 2007;16:3497–510.
96. Campos M, Hanemaaijer M, Gripkey H, Collier TC, Lee Y, Cornel AJ, et al. The origin of island populations of the African malaria mosquito, Anopheles coluzzii. Commun Biol. 2021;4.
97. Bergey CM, Lukindu M, Wiltshire RM, Fontaine MC, Kayondo JK, Besansky NJ. Assessing connectivity despite high diversity in island populations of a malaria mosquito. Evol Appl. 2020;13:417–31.
98. Lanzaro GC, Campos M, Crepeau M, Cornel A, Estrada A, Gripkey H, et al. Selection of sites for field trials of genetically engineered mosquitoes with gene drive. Evol Appl. 2021;14:2147–61.
99. Ellegren H, Galtier N. Determinants of genetic diversity. Nat Rev Genet. 2016;17:422–33.
100. Fischer MC, Rellstab C, Leuzinger M, Roumet M, Gugerli F, Shimizu KK, et al. Estimating genomic diversity and population differentiation - an empirical comparison of microsatellite and SNP variation in Arabidopsis halleri. BMC Genomics. 2017;18:1–15.
101. O'Loughlin SM, Magesa SM, Mbogo C, Mosha F, Midega J, Burt A. Genomic signatures of population decline in the malaria mosquito *Anopheles gambiae*. Malar J. 2016;15:1–10.
102. Lobo NF, Sangaré DM, Regier AA, Reidenbach KR, Bretz DA, Sharakhova M V., et al. Breakpoint structure of the *Anopheles gambiae* 2Rb chromosomal inversion. Malar J. 2010;9.
103. White BJ, Cheng C, Sangaré D, Lobo NF, Collins FH, Besansky NJ. The population genomics of trans-specific inversion polymorphisms in *Anopheles gambiae*. Genetics. 2009;183:275–88.
104. Petrarca V, Nugud AD, Elkarim Ahmed MA, Haridi AM, Di Deco MA, Coluzzi M. Cytogenetics of the Anopheles gambiae complex in Sudan, with special reference to An. arabiensis: Relationships with East and West African populations. Med Vet Entomol. 2000;14:149–64.
105. Peter Andolfatto, Frantz Depaulis AN. Inversion polymorhisms and nucleotide variability in Drosophila. Genetics Research Cambridge. 2001;77:1–8.
106. Hare MP, Nunney L, Schwartz MK, Ruzzante DE, Burford M, Waples RS, et al. Understanding and Estimating Effective Population Size for Practical Application in Marine Species Management. Conservation Biology. 2010. p. 438–49.
107. Waples RS, Do C. Linkage disequilibrium estimates of contemporary Ne using highly variable genetic markers: A largely untapped resource for applied conservation and evolution. Evol Appl. 2009;3:244–62.
108. Wang J. Estimation of effective population sizes from data on genetic markers. Philosophical Transactions of the Royal Society B: Biological Sciences. Royal Society; 2005. p. 1395–409.

109. Rousset F. Genetic differentiation and estimation of gene flow from F-statistics under isolation by distance. Genetics. 1997;145:1219–28.
110. Neafsey DE, Waterhouse RM. Highly evolvable malaria vectors: The genomes of 16 *Anopheles* mosquitoes. 2015 [cited 2024 Aug 12]; Available from: http://dx.doi.
111. Hoffmann AA, Willi Y. Detecting genetic responses to environmental change. Nat Rev Genet. 2008. p. 421–32.
112. Weetman D, Wilding CS, Neafsey DE, Müller P, Ochomo E, Isaacs AT, et al. Candidate-gene based GWAS identifies reproducible DNA markers for metabolic pyrethroid resistance from standing genetic variation in East African *Anopheles gambiae*. Sci Rep. 2018;8.
113. Athrey G, Hodges TK, Reddy MR, Overgaard HJ, Matias A, Ridl FC, et al. The Effective Population Size of Malaria Mosquitoes: Large Impact of Vector Control. PLoS Genet. 2012;8.
114. Charlesworth B. Effective population size and patterns of molecular evolution and variation. Nature Reviews|Genetics. 2009;10:195–205.
115. Yaro AS, Traoré AI, Huestis DL, Adamou A, Timbiné S, Kassogué Y, et al. Dry season reproductive depression of *Anopheles gambiae* in the Sahel. J Insect Physiol [Internet]. 2012;58:1050–9. Available from: http://dx.doi.org/10.1016/j.jinsphys.2012.04.002
116. White MT, Griffin JT, Churcher TS, Ferguson NM, Basáñez MG, Ghani AC. Modelling the impact of vector control interventions on *Anopheles gambiae* population dynamics. Parasit Vectors. 2011;4.
117. Kamdem C, Fouet C, Gamez S, White BJ. Pollutants and Insecticides Drive Local Adaptation in African Malaria Mosquitoes. Mol Biol Evol. 2017;34:1261–75.
118. Waples RS. Life-history traits and effective population size in species with overlapping generations revisited: The importance of adult mortality. Heredity (Edinb). 2016;117:241–50.
119. Mwima R, Hui TYJ, Kayondo JK, Burt A. The population genetics of partial diapause, with applications to the aestivating malaria mosquito *Anopheles coluzzii*. Mol Ecol Resour. 2024;24.
120. Mwima R, Hui TYJ, Nanteza A, Burt A, Kayondo JK. Potential persistence mechanisms of the major *Anopheles gambiae* species complex malaria vectors in sub-Saharan Africa: a narrative review. Malar J [Internet]. 2023 [cited 2024 Jun 24];22:1–12. Available from: https://malariajournal.biomedcentral.com/articles/10.1186/s12936-023-04775-0

1061 **Supplementary Information (SI)**

1062 **Table S1.** Nucleotide diversity and Tajima's D for the six *An. gambiae* populations. The last row

1063 is all *An. gambiae* (2918) combined for comparison. Site choice was as described in the main

1064 text. The asterisk * denotes statistical significance, ($p < 0.05$). † Denotes an island population.

Population	**Nucleotide diversity (π)**	**Tajima's D**
Kayonjo	0.01163	-2.3069*
Katuuso	0.01143	-2.0219*
Kibbuye	0.01169	-2.2356*
Kiimi †	0.01081	-0.8223
Kansambwe †	0.01071	-1.0827
Bugiri †	0.01103	-0.6954
All *An. gambiae* (Mainland & Island)	0.01150	-2.3073*

1065

1066 **Table S2.** Nucleotide diversity and Tajima's D for the three *An. arabiensis* populations

1067 The last row is all *An. arabiensis* (173) combined for comparison. Site choice was as described

1068 in the main text.

Population	**Nucleotide diversity (π)**	**Tajima's D**
Kayonjo	0.00859	-1.17475
Katuuso	0.00829	-0.98993
Kibbuye	0.00847	-1.73386
All *An. arabiensis*	0.00859	-1.91156

1069